Langmuir

Article

pubs.acs.org/Langmuir

Fabrication of Patterned Nanofibrous Mats Using Direct-Write Electrospinning

Jongwan Lee,[†,#] Seung Yong Lee,[†,#] Jinah Jang,[‡] Young Hun Jeong,[*,⊥] and Dong-Woo Cho[‡,§]

[†]Graduate School of Knowledge-Based Technology & Energy, Korea Polytechnic University, Gyeonggi 429-793, South Korea

[‡]Division of Integrative Biosciences and Biotechnology, POSTECH, Kyungbuk 790-784, South Korea

[§]Department of Mechanical Engineering, POSTECH, Kyungbuk 790-784, South Korea

[⊥]Department of Mechanical Engineering, Korea Polytechnic University, Gyeonggi 429-793, South Korea

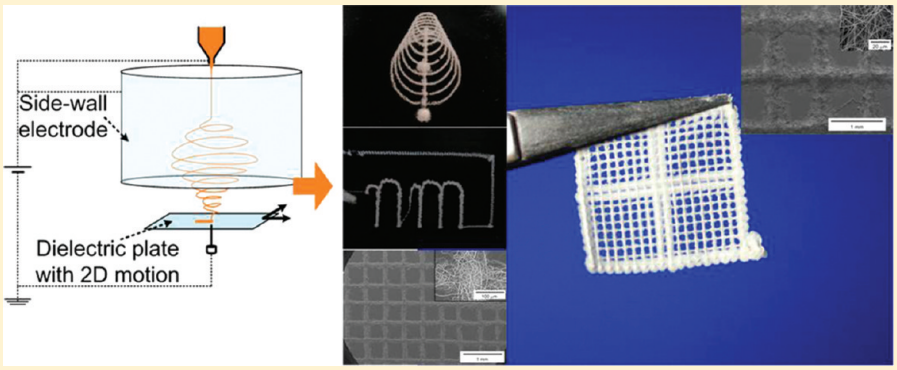

ABSTRACT: Due to the numerous advantages of nanofibers, there is a strong demand in various fields for nanofibrous structures fabricated by electrospinning. However, the process is currently beset by troublesome limitations with respect to geometric and morphological control of electrospun nanofibrous mats. This study presents a direct-write electrospinning process and apparatus with improved focusing and scanning functionalities for the fabrication of various patterned thick mats and nanofibrous patterns with high geometric fidelity, supported by a number of experimental results. Consequently, various patterned nanofibrous mats were fabricated using the developed method. Additionally, the fabricated mat was successfully used for cell patterning as a bioengineering application. The proposed method is expected to significantly improve the properties and functionalities of nanofibrous mats in a variety of applications.

Downloaded by ITESM at 07:53:48:959 on June 10, 2019
from https://pubs.acs.org/doi/10.1021/la3009249.

1. INTRODUCTION

Recently, there has been intensive use of nanofiber-based structures in various areas,[1,2] including reinforcement of composites, nano-, bio-, and tissue engineering,[3−6] filtration,[7] clothing, electronics, sensors, energy,[8−12] and drug delivery. Due to the significant advantages of their small diameter, large surface-area-to-volume ratio, high flexibility in surface functionality, and superior mechanical properties, nanofibers provide numerous opportunities to dramatically improve the performance of existing technologies/devices and to break new ground in a variety of fields.[1,13] In particular, thick nanofibrous mats are more valuable in scaffolds, drug carriers, and filters.

Electrospinning, which was originally proposed in 1934,[9] remains one of the most effective methods for manufacturing nanofibrous structures. The procedure is not limited to particular materials and thus can be applied to a wide range of fields. However, a number of issues need to be resolved; a particularly difficult one is control of the morphology and geometry of electrospun nanofibrous patterns and mats.[10,14] In general, electrospun nanofibers and mats have a highly random morphology, resulting from the whipping motion of the electrospinning jet.[15] Therefore, it has been difficult to improve the performance of applications by introducing specific morphological characteristics to a nanofibrous mat. The morphology of electrospun nanofibrous structures can be subdivided into the morphologies of single fibers and fibrous membranes/mats.[16] The diameters of single electrospun fibers vary from several nanometers to the micrometer scale and can be controlled by well-known process parameters.[16,17] The size of a membrane/mat is generally several millimeters to hundreds of millimeters. In this respect, electrospun patterns play a role as a bridge between single fibers (nano- and microscale structures) and the features of membranes/mats (macrostructures). Therefore, the control of electrospun patterns enables control of electrospun mat morphology and introduces various morphological functionalities such as specific mechanical properties.

Until now, research on the morphology of nanofibrous structures has mainly focused on the nanofiber alignment.[18−22] Although nanofiber alignment was a significant breakthrough for nanofibrous mats, the process is still hampered by some

Received: November 17, 2011
Published: April 18, 2012

 © 2012 American Chemical Society

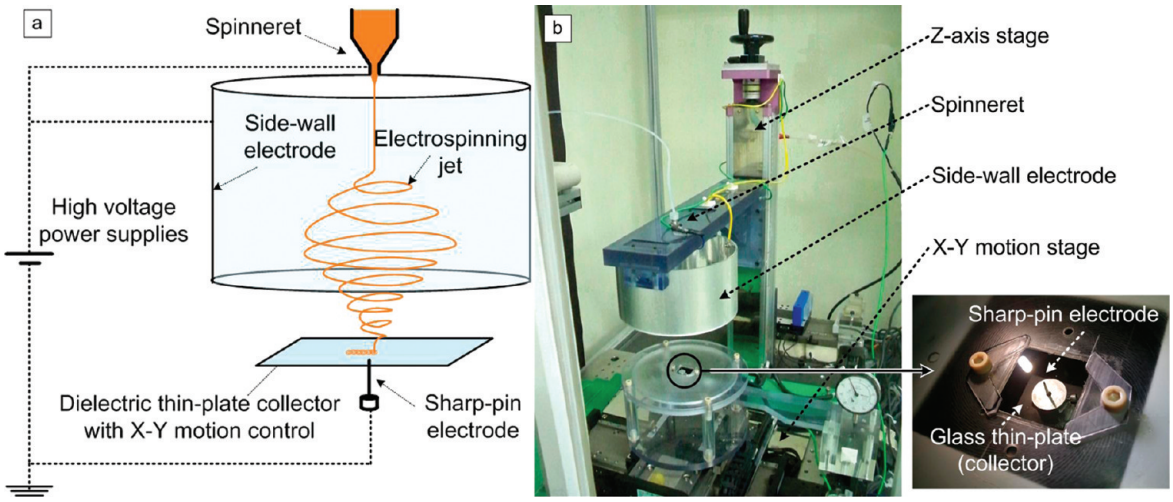

Figure 1. (a) Schematic of the direct-write electrospinning apparatus. (b) Actual experimental setup. A borosilicate glass plate with a thickness of about 100 μm was used as the collector.

troublesome limitations, such as the control of geometric features of the electrospun mats and the introduction of various geometrical functionalities. Another useful approach involves direct nanofiber patterning. An attractive method is to use a prepatterned conductive collector to obtain patterned nanofibrous structures.[23−26] Additionally, photolithography techniques have been successfully introduced to patterning electrospun nanofibrous membranes or mats.[27,28] These studies used prepatterned masks to pattern an electrospun nanofibrous layer for selective photo-cross-linking. Meanwhile, mechanical shearing using a pair of prepatterned micromolds has been proposed to avoid the need for a photoinitiator and the limitation of polymer material selection in the photolithography patterning.[29] Although these methods are practical and produce excellent results, the morphology of the nanofibrous membrane highly depends on prepatterned collectors/masks/molds, and the material selection is limited.

In this regard, direct-write deposition is a powerful solution to direct patterning of nanofibers. Several groups have reported that short tip-to-collector distance (TCD) and fast motion of the collector during the electrospinning process allows direct and precise deposition of nearly straight nanofibers.[30−33] However, this approach appears suitable for fabricating thin nanofibrous membranes and patterns rather than thick mats. Dalton et al. demonstrated that simple nanofibrous patterns with line widths as small as 500 μm can be fabricated via melt electrospinning with a larger TCD and lower speed, using a plate collector with two-dimensional (2D) motion.[14] Furthermore, Bellan and Craighead proposed a fascinating method using a secondary electrode for focusing and jet-steering.[34] However, these techniques have not shown sufficient capacity for direct writing of nanofibrous mats with high fidelity and controllability of geometry and size, which are critical issues to improve their performance and quality for various practical applications such as fuel cells, scaffolds, and filters.

In this work, we demonstrate that various nanofibrous patterns and patterned mats can be fabricated with high geometric fidelity using an improved electrospinning process that merges three concepts: conventional electrospinning, improved focusing, and scanning functions. In contrast to morphology control via fiber alignment, the proposed electrospinning process offers the following advantages. First, it retains the beneficial effects of highly random nanofiber connectivity, which resembles an extracellular matrix in biology[35] and can introduce micro- to nanoscale porosity to a structure. Second, we can obtain multilevel porosity, including pores that are intentionally generated by geometric patterns (for example, the lattices of pores shown in Figure 5), with sizes ranging from hundreds to tens of micrometers, and pores generated by the fiber connectivity. Third, nanofibrous 2D structures with various geometries can be fabricated. To enhance focusing performance, cylindrical side-wall and sharp-pin ground electrodes were used, as justified by a finite element analysis of the electric field. Also, to introduce scanning functionality, a dielectric thin plate with 2D motion was used as a collector capable of planar motion independent of the sharp-pin ground electrode. As a result, the geometry and size of electrospun fibers can be controlled by process parameters. Consequently, various nanofibrous patterns, including lines, points, lattices, and alphabetic characters, and lattice-patterned mats with various mesh sizes, can be successfully fabricated with high geometric fidelity using the developed system. In addition, we demonstrate a preliminary application of the fabricated nanofibrous mat to cell patterning, which could eventually be used for a scaffold, biosensor, or biofilter.

2. EXPERIMENTAL SECTION

Electrospinning Apparatus and Materials. The direct-writing approach[36,37] is one of the most attractive ways of fabricating nanofibrous patterns via electrospinning (in which a single fiber is generally spun out from a spinneret). To use this approach, two functions must be added to the conventional electrospinning apparatus: focusing the electrospinning jet on a point and scanning the collector along a predefined path.[16] In this way, nanofibrous patterns can be deposited by scanning an instantaneous point-like nanofiber deposition, which can be likened to the focused beam spot in electron beam lithography. The diameter of the instantaneous point-like deposition can be regarded as the width of the line/contour patterns, while the scan path corresponds to the pattern shape. Consequently, the geometric fidelity of an electrospun pattern is strongly dependent on the focusing quality and scan path.

To focus the electrospinning jet, a sharp-pin ground electrode and a cylindrical side-wall electrode were introduced, as shown in Figure 1a. As a result, the electric field lines can be directed and concentrated toward the ground electrode, causing the electrospinning jet to converge toward this electrode. A dielectric thin plate was used as a

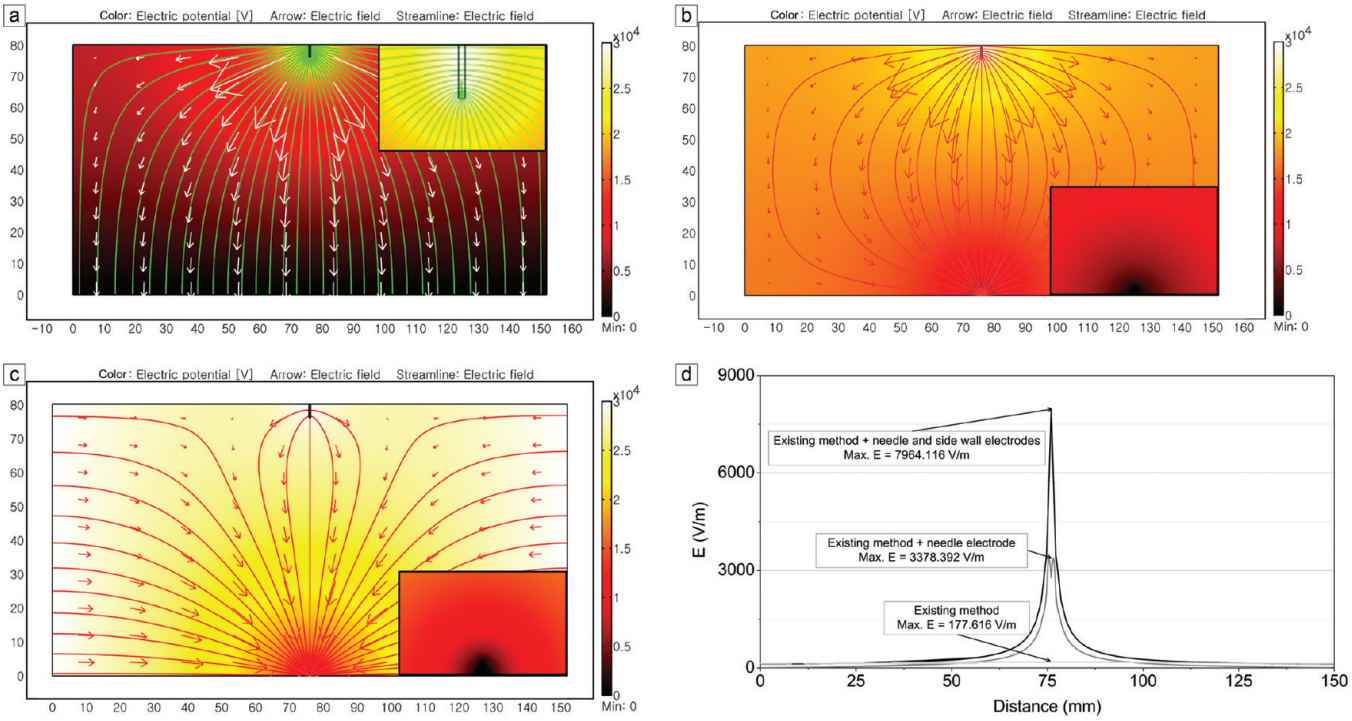

Figure 2. Electric field simulation results for the three electrospinning apparatus cases with the same tip-to-collector distance (TCD) of 76 mm and supplied voltage to the spinneret of 30 kV. The colors, arrows, and streamlines indicate the electric potential, electric field vector, and shape, respectively. (a) A conventional electrospinning apparatus with a collector plate. (b) An improved electrospinning apparatus with a sharp-pin ground electrode. (c) Proposed electrospinning apparatus equipped with a cylindrical side-wall electrode and a sharp-pin ground electrode. (d) Electric field strength distribution at the bottom plane, including the collectors, for the three cases.

collector to avoid interference with the focused electric field. To provide scanning functionality, the collector was placed directly above the fixed ground electrode and was capable of numerically controlled two-dimensional planar motion. As a result, nanofibers focused toward the ground electrode can be deposited on the collector along the scan path. The overall process is influenced by scan speed and dwell time, as well as the conventional electrospinning process parameters.

The experimental setup for the proposed method is shown in Figure 1b. The test system was composed of a high-voltage power supply, a syringe pump, a needle spinneret with an inner diameter of 200 μm, an aluminum-coated cylindrical side-wall electrode, a sharp-pin ground electrode, a 2D linear stage, and a thin borosilicate glass plate with a thickness of about 100 μm. The system was placed inside a chamber to isolate it from its surroundings. The TCD was adjusted using a manual stage. The distance between the collector plate and the ground electrode was maintained at about 50 μm, also using a precision manual stage. The side-wall electrode had the same voltage as the spinneret.

The polymer used for the electrospinning was a polycaprolactone with a number average molecular weight (M_n) between 70 000 and 90 000 (440744, Sigma-Aldrich, Co.). The polymer was dissolved in 99.5% pure chloroform (C0584, Samchun Pure Chemical Co., LTD) at a concentration of 8.8 wt % and stirred for 120 min to obtain a homogeneous solution.

Finite Element Analysis. We simulated the electric field of the proposed electrospinning apparatus using finite element analysis to demonstrate the effect of the introduced side-wall electrode and sharp-pin ground electrode on focusing nanofibers. The apparatus consisting of air, glass thin-plate, and electrodes such as a needle spinneret, a cylindrical side-wall electrode, and a sharp-pin ground electrode were modeled in 2D space. In the model, the diameter of the side-wall electrode was 150 mm. We constructed three models, consisting of a conventional electrospinning apparatus composed of a needle spinneret and a conductive plate collector, an improved apparatus with a sharp-pin ground electrode, and the proposed apparatus, to compare electric fields. We predicted the electric field for the three models under the same conditions of a 76 mm TCD and a 30 kV supplied voltage using the COMSOL Multiphysics simulation package.

Fabrication of Nanofibrous Thick Mats. During fabrication of nanofibrous patterns, nanofibers are electrospun along a predefined path on the collector, as described above. Therefore, a nanofibrous pattern can be obtained by scanning the collector along the path once (single-layer pattern). However, fabricating a nanofibrous thick mat requires increased pattern thickness. Thus, we employed a layer-by-layer approach to increase thickness. In this regard, the nanofibrous mat consisted of multiple layers of a nanofibrous pattern.

Heat treatment at 80 °C for 7 s was performed to improve the structural integrity of the electrospun mat before detachment from the collector plate. The heat-treated mat was detached from the collector plate after wetting with ethanol, and it was then dried to remove the solvent and the ethanol.

Morphological Observations and Dimension Measurement. The morphologies of the electrospun patterns and mats shown in Figures 3 and 4 were investigated by field-emission scanning electron microscopy (SEM; S4700, Hitachi Co), whereas the morphologies of the patterns and mats shown in Figure 5 and 6 were observed using another scanning electron microscope (Nova Nano 200, FEI). We measured the thickness and width of the nanofibrous line patterns with 1, 5, 10, 20, and 30 layers to investigate their geometric fidelity, as shown in Figure 4. We used both a noncontact surface profiler (New view 6300, Zygo Co.) and a contact surface profiler (Alpha-step IQ, KLA Tencor Co.) to measure thickness. The width was calculated from the SEM images.

Cell Live/Dead Assay. To demonstrate the capabilities of the fabricated nanofibrous mats for bioengineering, a fabricated patterned nanofibrous mat was used for cell patterning. This could be a preliminary step toward using the mats to produce a scaffold, biosensor, or biofilter. A cell viability test was conducted using live/dead viability staining to demonstrate cell patterning using a fabricated nanofibrous mat. A mouse embryonic fibroblast cell line (NIH3T3) was seeded onto both a patterned mat with a grid size of 0.3 × 0.3 mm^2 fabricated by the proposed process and a randomly deposited

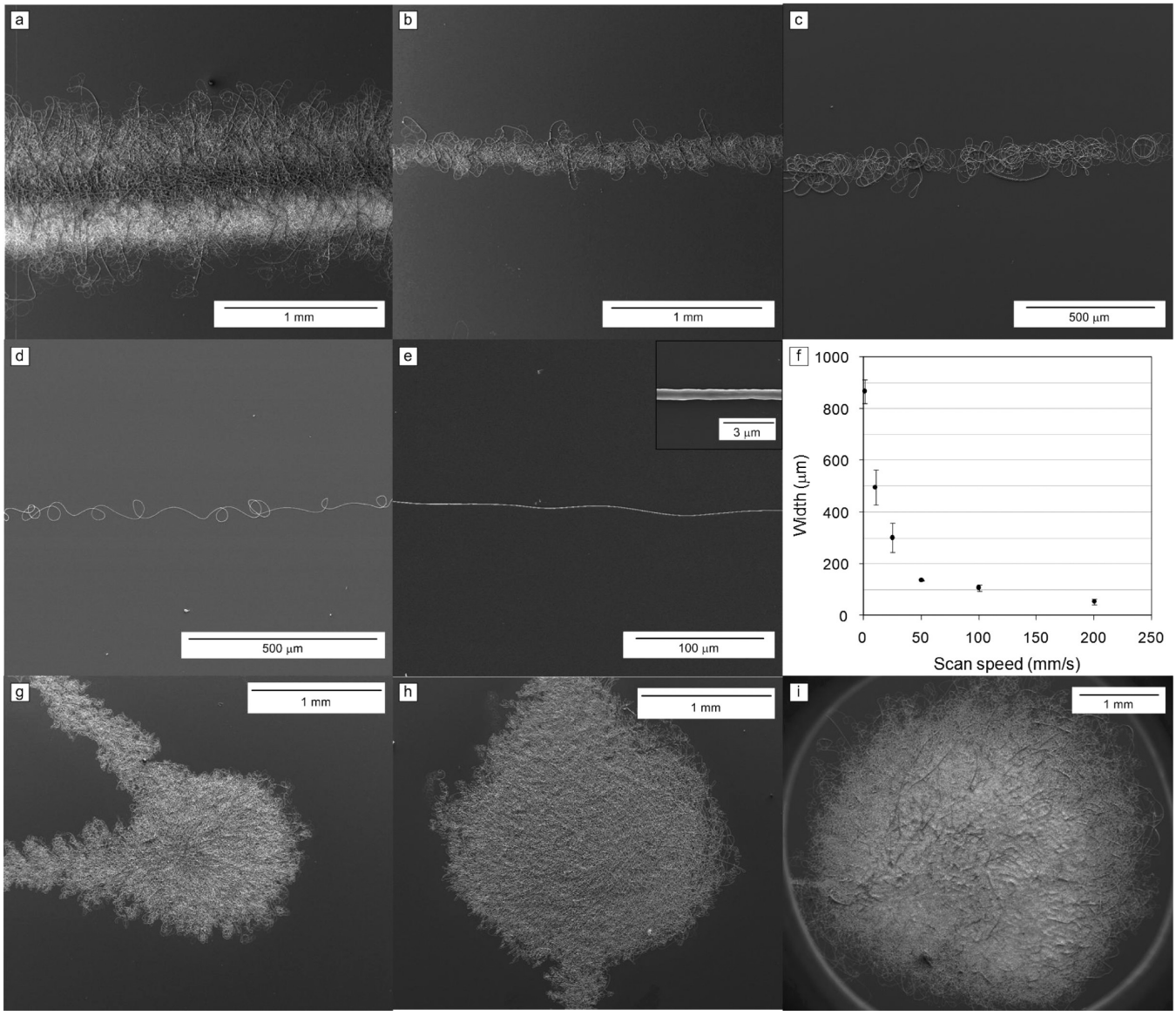

Figure 3. Line pattern for a scan speed of (a) 2 mm/s, (b) 25 mm/s, (c) 100 mm/s, (d) 200 mm/s, and (e) 500 mm/s. The fiber diameter was 641 nm, as shown in the inset. (f) Relationship between the width of the electrospun line pattern and the scan speed of the collector plate. Point pattern for a dwell time of (g) 0.5 s, (h) 1 s, and (i) 10 s.

nanofibrous mat fabricated by the conventional electrospinning process at a density of 4×10^5 cells/cm^2. After a 4 h culture at 37 °C, the cell-seeded mats were cultured in DMEM supplemented with 10% fetal bovine serum, 100 U/mL penicillin, and 100 μg/mL streptomycin to attach cells. Cell viability on the mats was determined using a live/dead viability kit (L-3224; Molecular Probes, Eugene, OR), and they were imaged using a confocal microscope (LSM 510 Meta, Carl Zeiss). Green fluorescence by calcein AM indicated live cells, whereas red fluorescence by the ethidium homodimer indicated dead cells.

■ RESULTS AND DISCUSSION

Electric Field Simulation. Figure 2a−c shows the predicted electric field distribution for three cases: a conventional electrospinning apparatus with a ground plate, an improved electrospinning apparatus with a sharp-pin ground electrode, and the proposed electrospinning apparatus. As shown in Figure 2a, the electric field in the conventional electrospinning apparatus had a uniform distribution near the ground plate, indicating that the attraction force for nanofibers was uniform over the plate. Therefore, nanofibers could be deposited randomly anywhere on the plate. In Figure 2b,c, the electric field lines are directed and concentrated toward the sharp-pin electrode, which caused the electrospinning jet to converge toward this electrode. However, the envelope of the electric field line in Figure 2c is narrower than that in Figure 2b, which results from the repulsive effect of the side-wall electrode. As a result, the electrospinning jet was effectively focused toward the sharp-pin electrode. Figure 2d shows electric field strength along the bottom plane, which was proportional to the electric field force,[38] including the collectors, for the three cases. The maximum electric field strengths of the three cases were 117.616, 3378.392, and 7964.116 V/m, respectively. The maximum electric field strength in the proposed apparatus was 67.71 times higher than that of the conventional apparatus (Figure 2a). Moreover, the distribution of electric field strength at the bottom plain had a sharp cone shape, which provided higher selectivity for nanofiber deposition. Therefore, the proposed method

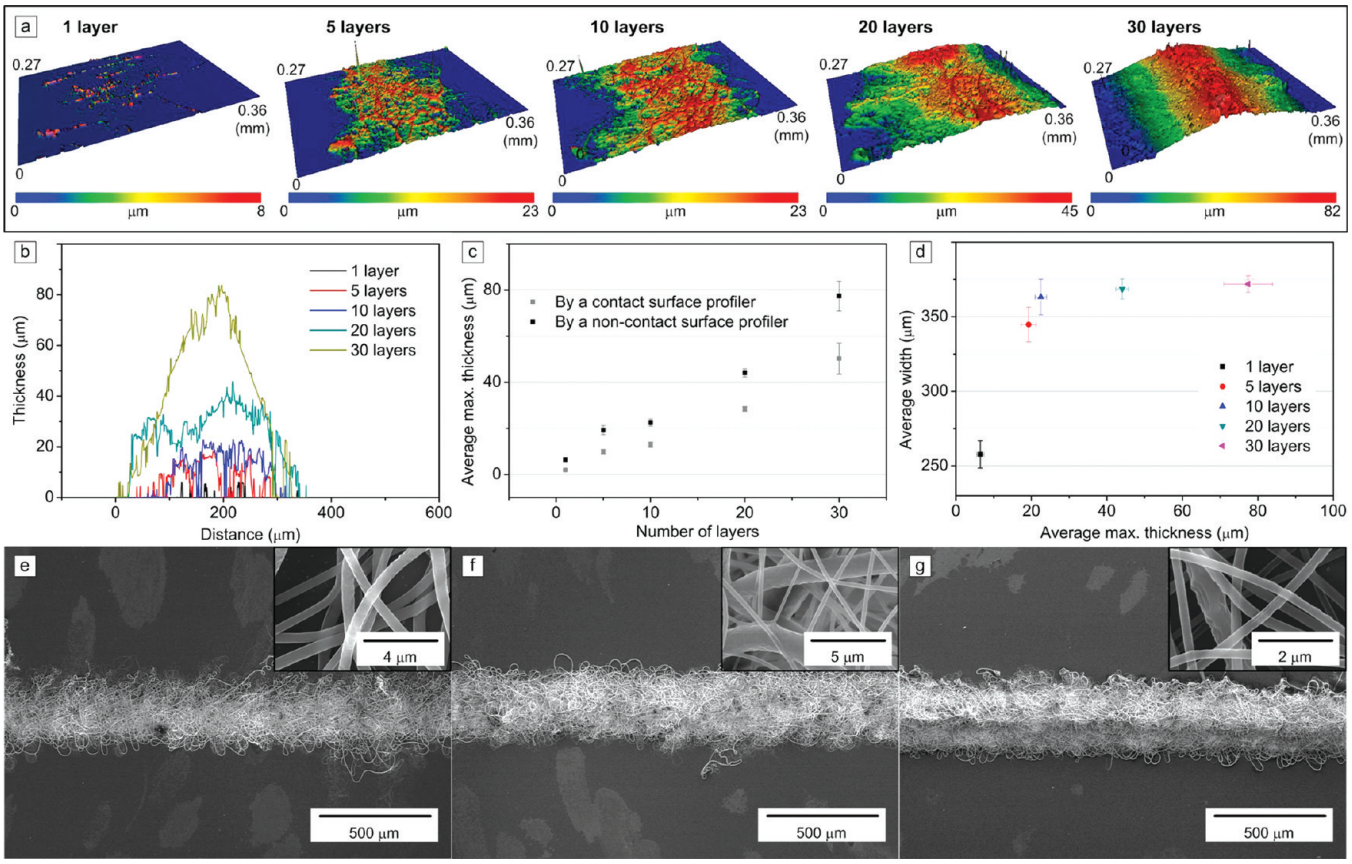

Figure 4. (a) Three-dimensional measurement of nanofibrous line patterns with 1, 5, 10, 20, and 30 layers using a noncontact surface profiler. (b) Cross-section profiles of the nanofibrous line patterns measured by a noncontact surface profiler. (c) Relationship between the number of layers and the line pattern thickness measured by a contact surface profiler (black symbols) and a noncontact surface profiler (gray symbols). (d) Relationship between the thickness and width of the nanofibrous line pattern with respect to the number of layers. (e−g) Scanning electron micrograph images of 10-, 20-, and 30-layer nanofibrous line patterns, respectively.

achieved significantly higher focusing quality of the nanofibers than that of the other methods.

Control of Feature Size. There are a number of environmental factors that influence the electrospinning process, such as temperature, humidity, and pressure, as well as processing parameters, such as flow rate, solution concentration, and electric field.[16] The proposed method is also affected by the collector motion parameters, such as dwell time and scan speed. Thus, we experimentally[35,39−41] investigated the relationships between feature size and collector motion parameters to demonstrate the controllability of feature size. As experimental conditions, the electrical voltage was 25 kV and the TCD was about 70 mm. In particular, the ratio of electrical voltage to TCD was much higher than that of existing studies due to the presence of the glass plate collector and cylindrical side-wall electrode. The flow rate of the solution was set at 0.1 mL/h. During the experiments, the temperature was maintained at about 23 °C, and the relative humidity was between 54% and 57%. The scan speed of the collector was varied from 2 to 200 mm/s to identify the relationship between the width of the line pattern and the scan speed. Figure 3a−d shows the line patterns fabricated under the given conditions. In Figure 3a, the scan speed was 2 mm/s and the width of the line pattern was about 950 μm. Figure 3b−d shows the line patterns fabricated when the collector moved at scan speeds of 25, 100, and 200 mm/s, respectively. These values indicate that the nanofibers were deposited with a well-defined line width along the scan path. Various fiber diameters from about 400 nm to 4 μm were observed. Under low-speed conditions, the nanofibers were densely deposited, as shown in Figure 3a, while higher-speed collector motions induced sparser deposition. In particular, under the given process and environmental conditions, a single straight nanofiber pattern with a fiber diameter of 641 nm was obtained when the scan speed was 500 mm/s, as shown in Figure 3e. Consequently, Figure 3f shows that the line width was inversely proportional to the scan speed of the collector plate. We investigated the influence of dwell time on the diameter of the point pattern electrospun under the conditions cited above. Figure 3g−i shows the point patterns fabricated for dwell times of 0.5, 1, and 10 s between two line segment motions. These figures indicate that the diameter of the circular point pattern increased to 4 mm as the dwell time increased to 10 s. In the experiments, the morphology of an individual nanofiber was similar to that shown in Figure 3a−e. From Figure 3a−i, it can be concluded that the dimensions of primitive geometries, such as line and point patterns, can be controlled by adjusting the motion parameters, as well as the conventional process parameters.

As described above, the layer-by-layer approach was employed to fabricate the nanofibrous thick mats. Therefore, we investigated the effect of the number of layers on the geometric fidelity of the patterns. Figure 4a shows the three-dimensional morphology of the nanofibrous line patterns with 1, 5, 10, 20, and 30 layers. During fabrication of these patterns,

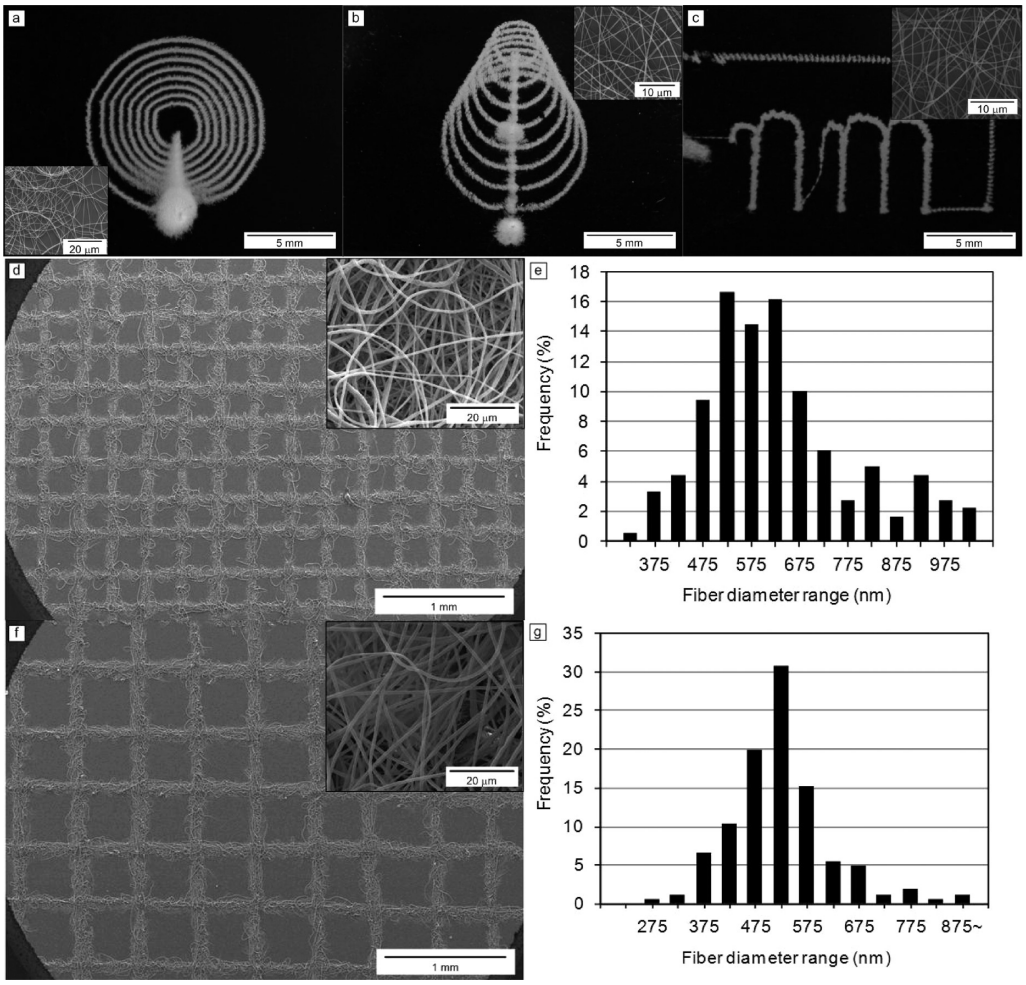

Figure 5. (a) Photograph of a nanofibrous pattern consisting of a set of concentric circles with a maximum radius of 5 mm. (b) Photograph of a pattern composed of stepwise reduced and shifted circles with a maximum radius of 5 mm. (c) Photograph of a pattern consisting of the alphabetic characters "nm". (d) Scanning electron micrograph (SEM) image and (e) fiber diameter distribution of a membrane with a single-layer lattice pattern and a grid size of 0.3 × 0.3 mm^2 (f) SEM images and (g) fiber diameter distribution of lattice pattern membranes with a grid size of 0.5 × 0.5 mm^2. The fabrication times for the circular and alphabetic patterns a–c were 13.2, 13.5, and 3.3 s, respectively. The total fabrications times for the membranes shown in d and e were 174 and 101 s, respectively.

the scan speed, voltage, TCD, concentration, and flow rate of the solution were 33.3 mm/s, 29.5 kV, 60 mm, 8.8 wt %, and 0.1 mL/h, respectively; these were identical to the fabrication conditions for the thick mats shown in Figure 6. As shown in Figure 4a, the line pattern thickness and nanofiber density increased as the number of layers became larger. Additionally, the pattern cross-section became similar to a mountain-shape, as shown in Figure 4b, which shows the cross-sectional profiles of the patterns as measured by a noncontact surface profiler. Figure 4c compares the change in the maximum thickness of the pattern according to the number of layers measured by the noncontact profiler and the contact profiler to verify the results, because a noncontact measurement of a nanofibrous structure is susceptible to interference. Here, however, the noncontact measurement results resembled the contact measurement results with a small difference due to the contact force compression. We concluded that the thickness of the pattern can be controlled by the number of layers.

The relationship between the average width and thickness of the nanofibrous line pattern is shown in Figure 4d. The line pattern width increased significantly up to 10 layers (344.82 μm); however, it varied little after 10 layers. In particular, the width change between the 10- and 30-layer patterns was <2.4%, as shown in Figure 4e–g. Therefore, the layer-by-layer approach using the proposed electrospinning apparatus effectively increased the pattern thickness without loss of geometric fidelity during fabrication of a patterned nanofibrous mat.

Fabrication of Various Nanofibrous Patterns. Nanofibrous patterns with a variety of geometries and morphological characteristics were fabricated via the proposed direct-write electrospinning process under various experimental conditions. Figure 5a–c shows complex patterns of circles and the alphabetic characters "nm", which were electrospun under specific conditions at a voltage of 30 kV, a TCD of 80 mm, and a flow rate of 0.05 mL/h. During the experiments, the relative humidity was maintained at about 56% and the temperature at 23 °C. Under these conditions, most of the electrospun nanofibers were between 300 and 700 nm. Patterns consisting of a set of concentric circles and a set of stepwise reduced and shifted circles, both with a maximum radius of 5 mm, were successfully fabricated at a scan speed of 150 mm/s, as shown in Figure 5a,b. A pattern of alphabetic characters with a line width of 370 μm was fabricated at a scan speed of 100 mm/s, as

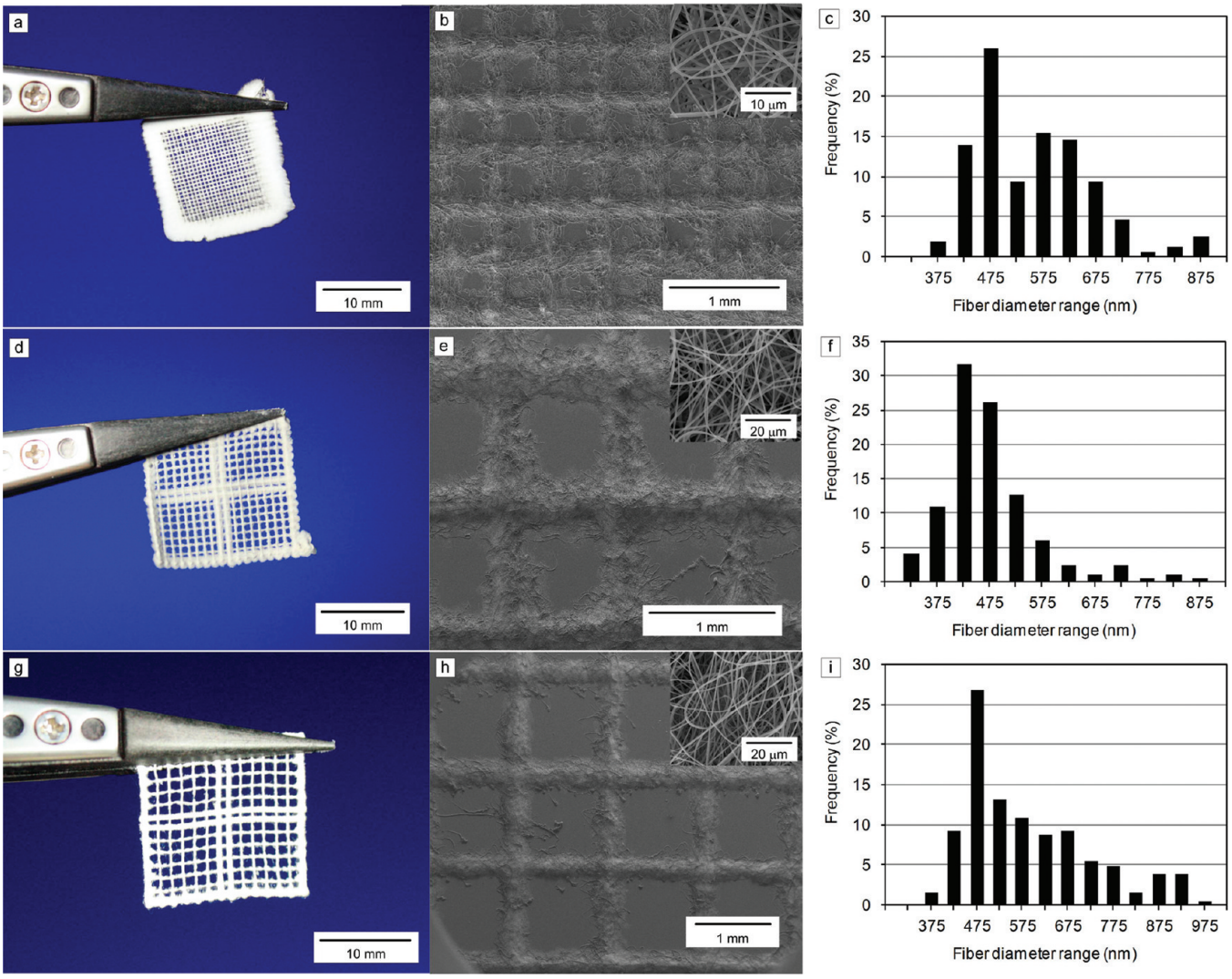

Figure 6. (a and b) Photograph, scanning electron micrograph, and (c) fiber diameter distribution of a lattice-patterned 10-layer mat with a grid size of 0.5 × 0.5 mm^2 and thickness of 41 μm. (d and e) Photograph, scanning electron micrograph, and (f) fiber diameter distribution of a lattice-patterned 30-layer mat with a grid size of 1.0 × 1.0 mm^2. (g and h) Photograph, scanning electron micrograph, and (i) fiber diameter distribution of a lattice-patterned 30-layer mat with a grid size of 1.3 × 1.3 mm^2. The mats in d and g had thicknesses of 72 μm. The fabrication times for the patterned nanofibrous mats shown in a, d, and g were 1080, 1110, and 900 s, respectively.

shown in Figure 5c. Two well-arranged single-layer membranes with rectangular lattice patterns and grid sizes of 0.3 × 0.3 and 0.5 × 0.5 mm^2 were also fabricated, as shown in Figure 5d and 5f. During fabrication of these membranes, the voltage, TCD, concentration, and flow rate of the solution, relative humidity, and temperature were 29.5 kV, 60 mm, 8.8 wt %, 0.1 mL/h, 55%, and 21.5 °C, respectively. Higher focusing performance was achieved under these conditions; thus, the line width was reduced to 100 μm when the scan speed was 25 mm/s. As a result, the average sizes of the membrane pores were 0.19 × 0.22 and 0.39 × 0.37 mm^2, respectively. As indicated in Figure 5e and 5g, the diameters of nanofibers composing the membranes shown in Figure 5d and 5f ranged from 525 to 625 nm, and from 475 to 575 nm, respectively.

Fabrication of Lattice Patterned Mats. We fabricated three nanofibrous mats with rectangular lattice patterns using the proposed direct-write electrospinning procedure. Figure 6a,b shows the fabricated mat consisting of 10 layers of the pattern indicated in Figure 5f. The mat had a grid size of 0.5 × 0.5 mm^2 and was fabricated under the same conditions as for the lattice pattern in Figure 5f. The size of the entire mat area was 17 × 17 mm^2. As Figure 5f and 6b indicates, the average size of the rectangular pores decreased significantly from about 0.39 × 0.37 to 0.20 × 0.22 mm^2 due to increased line pattern width, although the line pitch of both the patterns and mats remained at 494 μm. The thickness of the mat was 41 μm. Figure 6d and 6g shows the 30-layer mats, which were 18 × 18 mm^2. The dwell time was shortened from 500 to 70 ms to reduce the side-frame width. Additionally, the scan speed was increased from 25 to 33.3 mm/s. The mat in Figure 6d,e had a grid size of 1.0 × 1.0 mm^2 and an average pore size of 0.61 × 0.59 mm^2, whereas that of Figure 6g,h had a grid size of 1.3 × 1.3 mm^2 and an average pore size of 0.90 × 0.99 mm^2. The detached mats in Figure 6d and 6g had a thickness of 72 μm. The nanofibers that composed the mats in Figure 6b, 6e, and 6h were intensively distributed, with diameters ranging from 425 to 475 nm, 425 to 525 nm, and 475 to 525 nm, respectively, as shown in Figure 6c, 6f, and 6i. The diameters of the nanofibers that made up the membranes in Figure 6a, 6d,

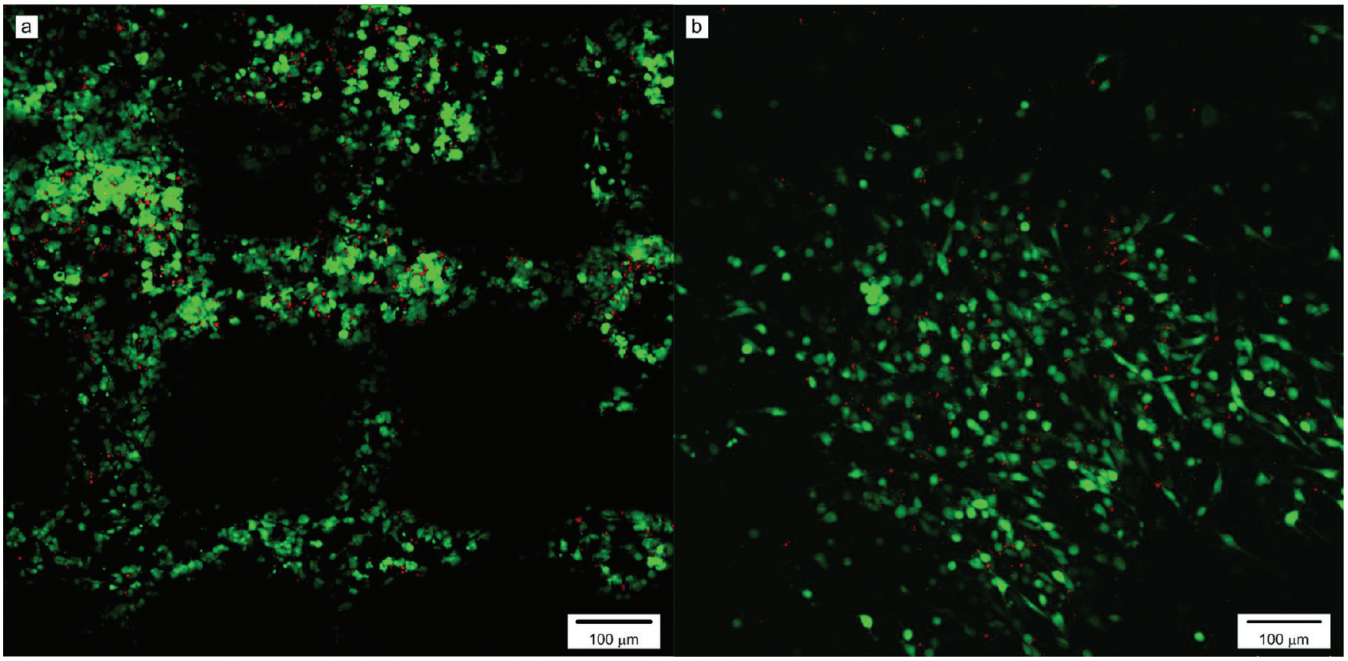

Figure 7. Confocal microscopy images of cell patterning on (a) a lattice-patterned nanofibrous mat using the proposed electrospinning apparatus as in Figure 5a and (b) a randomly deposited nanofibrous mat using the existing electrospinning apparatus. The green dots are live cells, and the red dots are dead cells.

and 6g ranged from 425 to 475 nm, 425 to 525 nm, and 475 to 525 nm, respectively.

Cell Patterning Using a Patterned Nanofibrous Mat. A fabricated patterned nanofibrous mat with a grid size of 0.5 × 0.5 mm^2, shown in Figure 6a, and a random deposited mat were used for cell patterning.[42,43] Before observation of live/dead cells on the nanofibrous mats, the mat was detached from the thin dielectric plate and placed on a glass cover. About 24 h after seeding of NIH3T3 cells, the live/dead cell assay showed that most of the seeded cells on the nanofibrous patterned mat using the proposed electrospinning apparatus (Figure 7a) and the randomly deposited nanofibrous mat using the existing electrospinning apparatus (Figure 7b) were still alive. Cells seeded on the randomly deposited nanofibrous mat had no distinguishing attachment direction, whereas cells seeded on the nanofibrous patterned mat were attached along the patterns. The size, shape, and morphology of the nanofibrous patterned mat, which demonstrated excellent cell viability in this study, will be used in the future for a cell-patterning study.

■ CONCLUSIONS

In summary, we developed a direct-write electrospinning process with improved focusing and scanning functionalities for generating various nanofibrous mats with high geometric fidelity. This procedure is able to overcome the limitations of existing approaches, which are hampered by difficulties in controlling the pore size and geometry as well as the morphologies of electrospun nanofibrous mats. We demonstrated that the proposed direct-write electrospinning method could control the geometry and dimensions of nanofibrous patterns and mats via several fabrication examples. Additionally, the fabricated nanofibrous mats could be used in bioengineering, supported by a preliminary example of cell patterning. We anticipate that the new technique will lead to significantly improved control of the properties and functionalities of nanofibrous mats for a variety of applications.

■ AUTHOR INFORMATION

Corresponding Author

*Tel: 82-31-8041-0415. Fax: 82-31-8041-0419. E-mail: yhjeong@kpu.ac.kr.

Author Contributions

[#]These authors contributed equally to this work.

Notes

The authors declare no competing financial interest.

■ ACKNOWLEDGMENTS

This work was supported by the National Research Foundation of Korea (NRF) grant funded by the Korea government (MEST) (No. 2011-0000412).

■ REFERENCES

(1) Dzenis, Y. Spinning continuous fibers for nanotechnology. *Science* **2004**, *304* (5679), 1917.

(2) Lu, X.; Wang, C.; Wei, Y. One-Dimensional Composite Nanomaterials: Synthesis by Electrospinning and Their Applications. *Small* **2009**, *5* (21), 2349.

(3) Bhattarai, S. R.; Bhattarai, N.; Yi, H. K.; Hwang, P. H.; Cha, D. I.; Kim, H. Y. Novel biodegradable electrospun membrane: scaffold for tissue engineering. *Biomaterials* **2004**, *25* (13), 2595.

(4) Wnek, G. E.; Carr, M. E.; Simpson, D. G.; Bowlin, G. L. Electrospinning of nanofiber fibrinogen structures. *Nano Lett.* **2003**, *3* (2), 213.

(5) Yang, D.; Niu, X.; Liu, Y.; Wang, Y.; Gu, X.; Song, L.; Zhao, R.; Ma, L.; Shao, Y.; Jiang, X. Electrospun nanofibrous membranes: a novel solid substrate for microfluidic immunoassays for HIV. *Adv. Mater.* **2008**, *20* (24), 4770.

(6) Zong, X.; Bien, H.; Chung, C. Y.; Yin, L.; Fang, D.; Hsiao, B. S.; Chu, B.; Entcheva, E. Electrospun fine-textured scaffolds for heart tissue constructs. *Biomaterials* **2005**, *26* (26), 5330.

(7) Gopal, R.; Kaur, S.; Ma, Z.; Chan, C.; Ramakrishna, S.; Matsuura, T. Electrospun nanofibrous filtration membrane. *J. Membr. Sci.* **2006**, *281* (1−2), 581.

(8) Choi, S. W.; Jo, S. M.; Lee, W. S.; Kim, Y. R. An electrospun poly (vinylidene fluoride) nanofibrous membrane and its battery applications. *Adv. Mater.* **2003**, *15* (23), 2027.
(9) Huang, Z. M.; Zhang, Y. Z.; Kotaki, M.; Ramakrishna, S. A review on polymer nanofibers by electrospinning and their applications in nanocomposites. *Compos. Sci. Technol.* **2003**, *63* (15), 2223.
(10) Miao, J.; Miyauchi, M.; Simmons, T. J.; Dordick, J. S.; Linhardt, R. J. Electrospinning of Nanomaterials and Applications in Electronic Components and Devices. *J. Nanosci. Nanotechnol.* **2010**, *10* (9), 5507.
(11) Wu, J. J.; Chen, Y. R.; Liao, W. P.; Wu, C. T.; Chen, C. Y. Construction of Nanocrystalline Film on Nanowire Array via Swelling Electrospun Polyvinylpyrrolidone-Hosted Nanofibers for Use in Dye-Sensitized Solar Cells. *ACS Nano* **2010**, *4* (10), 5679.
(12) Langer, R. New methods of drug delivery. *Science* **1990**, *249* (4976), 1527.
(13) Agarwal, S.; Greiner, A.; Wendorff, J. H. Electrospinning of manmade and biopolymer nanofibers—Progress in techniques, materials, and applications. *Adv. Funct. Mater.* **2009**, *19* (18), 2863.
(14) Dalton, P. D.; Joergensen, N. T.; Groll, J.; Moeller, M. Patterned melt electrospun substrates for tissue engineering. *Biomed. Mater.* **2008**, *3*, 034109.
(15) Shin, Y.; Hohman, M.; Brenner, M.; Rutledge, G. Experimental characterization of electrospinning: the electrically forced jet and instabilities. *Polymer* **2001**, *42* (25), 09955.
(16) Ma, Z.; Kotaki, M.; Inai, R.; Ramakrishna, S. Potential of nanofiber matrix as tissue-engineering scaffolds. *Tissue Eng.* **2005**, *11* (1−2), 101.
(17) Fridrikh, S. V.; Yu, J. H.; Brenner, M. P.; Rutledge, G. C. Controlling the fiber diameter during electrospinning. *Phys. Rev. Lett.* **2003**, *90* (14), 144502.
(18) Katta, P.; Alessandro, M.; Ramsier, R.; Chase, G. Continuous electrospinning of aligned polymer nanofibers onto a wire drum collector. *Nano Lett.* **2004**, *4* (11), 2215.
(19) Li, D.; Wang, Y.; Xia, Y. Electrospinning Nanofibers as Uniaxially Aligned Arrays and Layer by Layer Stacked Films. *Adv. Mater.* **2004**, *16* (4), 361.
(20) Sundaray, B.; Subramanian, V.; Natarajan, T.; Xiang, R. Z.; Chang, C. C.; Fann, W. S. Electrospinning of continuous aligned polymer fibers. *Appl. Phys. Lett.* **2004**, *84*, 1222.
(21) Teo, W.; Kotaki, M.; Mo, X.; Ramakrishna, S. Porous tubular structures with controlled fibre orientation using a modified electrospinning method. *Nanotechnology* **2005**, *16*, 918.
(22) Yang, D.; Lu, B.; Zhao, Y.; Jiang, X. Fabrication of aligned fibrous arrays by magnetic electrospinning. *Adv. Mater.* **2007**, *19* (21), 3702.
(23) Cho, S. J.; Kim, B.; An, T.; Lim, G. Replicable Multilayered Nanofibrous Patterns on a Flexible Film. *Langmuir* **2010**, *26* (18), 14395.
(24) Yan, G.; Yu, J.; Qiu, Y.; Yi, X.; Lu, J.; Zhou, X.; Bai, X. Self-Assembly of Electrospun Polymer Nanofibers: A General Phenomenon Generating Honeycomb-Patterned Nanofibrous Structures. *Langmuir* **2011**, *27* (8), 4285.
(25) Zhang, D.; Chang, J. Patterning of electrospun fibers using electroconductive templates. *Adv. Mater.* **2007**, *19* (21), 3664.
(26) Zhang, D.; Chang, J. Electrospinning of three-dimensional nanofibrous tubes with controllable architectures. *Nano Lett.* **2008**, *8* (10), 3283.
(27) Carlberg, B.; Wang, T.; Liu, J. Direct photolithographic patterning of electrospun films for defined nanofibrillar micro-architectures. *Langmuir* **2010**, *26* (4), 2235.
(28) Sharma, C. S.; Sharma, A.; Madou, M. Multiscale carbon structures fabricated by direct micropatterning of electrospun mats of SU-8 photoresist nanofibers. *Langmuir* **2010**, *26* (4), 2218.
(29) Jao, P. F.; Machado, M.; Cheng, X.; Senior, D. E.; Kim, G. J.; Ding, D.; Sun, W.; Yoon, Y. K. Fabrication of nanoporous membrane and its nonlithographic patterning using Electrospinning and Stamp-thru-mold (ESTM). *Proceedings of The 24th IEEE International Conference on Micro Electro Mechanical Systems (MEMS 2011)*, Cancun, Mexico, Jan 23−27, 2011.
(30) Chang, C.; Limkrailassiri, K.; Lin, L. Continuous near-field electrospinning for large area deposition of orderly nanofiber patterns. *Appl. Phys. Lett.* **2008**, *93*, 123111.
(31) Hellmann, C.; Belardi, J.; Dersch, R.; Greiner, A.; Wendorff, J.; Bahnmueller, S. High precision deposition electrospinning of nanofibers and nanofiber nonwovens. *Polymer* **2009**, *50* (5), 1197.
(32) Kameoka, J.; Craighead, H. Fabrication of oriented polymeric nanofibers on planar surfaces by electrospinning. *Appl. Phys. Lett.* **2003**, *83* (2), 371.
(33) Sun, D.; Chang, C.; Li, S.; Lin, L. Near-field electrospinning. *Nano Lett.* **2006**, *6* (4), 839.
(34) Bellan, L. M.; Craighead, H. Control of an electrospinning jet using electric focusing and jet-steering fields. *J. Vac. Sci. Technol. B: Microelectron. Nanometer Struct.--Process., Meas., Phenom.* **2006**, *24*, 3179.
(35) Kolambkar, Y. M.; Dupont, K. M.; Boerckel, J. D.; Huebsch, N.; Mooney, D. J.; Hutmacher, D. W.; Guldberg, R. E. An alginate-based hybrid system for growth factor delivery in the functional repair of large bone defects. *Biomaterials* **2011**, *32*, 65.
(36) Chrisey, D. B. The power of direct writing. *Science* **2000**, *289* (5481), 879.
(37) Piner, R. D.; Zhu, J.; Xu, F.; Hong, S.; Mirkin, C. A. "Dip-pen" nanolithography. *Science* **1999**, *283* (5402), 661.
(38) Ramakrishna, S.; Fujihara, K.; Teo, W.-E.; Lim, T.-C.; Ma, Z. *An introduction to electrospinning and nanofibers*; World Scientific Pub. Co., Inc.: Singapore, 2005.
(39) Catledge, S.; Clem, W.; Shrikishen, N.; Chowdhury, S.; Stanishevsky, A.; Koopman, M.; Vohra, Y. An electrospun triphasic nanofibrous scaffold for bone tissue engineering. *Biomed. Mater.* **2007**, *2*, 142.
(40) Kim, C. H.; Khil, M. S.; Kim, H. Y.; Lee, H. U.; Jahng, K. Y. An improved hydrophilicity via electrospinning for enhanced cell attachment and proliferation. *J. Biomed. Mater. Res., Part B* **2006**, *78* (2), 283.
(41) Kim, G. H. Electrospun PCL nanofibers with anisotropic mechanical properties as a biomedical scaffold. *Biomed. Mater.* **2008**, *3*, 025010.
(42) Roth, E. A.; Xu, T.; Das, M.; Gregory, C.; Hickman, J. J.; Boland, T. Inkjet printing for high-throughput cell patterning. *Biomaterials* **2004**, *25* (17), 3707.
(43) Suh, K. Y.; Seong, J.; Khademhosseini, A.; Laibinis, P. E.; Langer, R. A simple soft lithographic route to fabrication of poly (ethylene glycol) microstructures for protein and cell patterning. *Biomaterials* **2004**, *25* (3), 557.